Revealing new opportunities with a cost-effective towed-streamer MAZ solution in the South Viking Graben, Norway

Julien Oukili[1], Luca Limonta[1], Martin Bubner[1], Eric Mueller[1] and Terje Kultom Karlsen[1] provide a fresh look at a new MAZ streamer concept that challenges existing multi-azimuth solutions, including OBS surveys, as it delivers a higher-quality dataset at a fraction of the cost and reduced environmental impact.

An integrated acquisition and imaging solution

In the autumn of 2019, a novel towed-streamer multi-azimuth (MAZ) acquisition and imaging concept, referred to as GeoStreamer X, was launched with the ambition to challenge existing seabed solutions in terms of overall costs and turnaround, as well as to deliver the highest achievable imaging quality for interpretation that may be obtained using one or more alternative solutions. We aim to demonstrate how all the survey design elements fall into place at the processing and velocity model building stages, in order to provide reliable images and pre-stack attributes, thereby emphasizing the benefit of an integrated acquisition and imaging approach.

The pilot study was conducted in the southern Viking Graben, a part of the North Sea Jurassic rift system which hosts a number of plays that have proven to be successful throughout decades of exploration. Hydrocarbons have been discovered in structural, stratigraphic and combination traps with Eocene-Paleocene sands and Jurassic-Triassic clastic reservoir targets. Recently, new exploration concepts have opened new plays such as Paleogene injectites, Upper Jurassic sands, Zechstein carbonates, and the fractured/weathered basement. However, the variety of exploration targets also introduces multiple subsurface imaging challenges. These challenges range from shallow subsurface channels and glacial features, Tertiary low velocity anomalies and high velocity sand injectites (V-brights), to multiple contamination in the polygonal faulted Paleogene and below the high impedance rugose Chalk. Figure 1 illustrates an overview of the main structural elements in the area with a full section display and key geological markers.

The 2019 pilot programme (Widmaier et al., 2020) added two new acquisition directions to an area already covered by a 3D multisensor towed-streamer survey from 2011, as shown on Figure 2. Naturally the sail line directions were set at 60 degrees relative angle to provide optimal azimuthal coverage. The new configurations used a 12 × 6000 m × 85 m (number of streamers, cable length, cable separation) high-density streamer spread, including two 10km-long streamer tails for Full Waveform Inversion (FWI) work, and a wide-towed triple source with 225 m separation between outer source arrays to improve the near offset coverage. This solution builds on the success of the flexible towing capabilities of PGS' high-capacity streamer vessels. Variable streamer length configurations have previously been
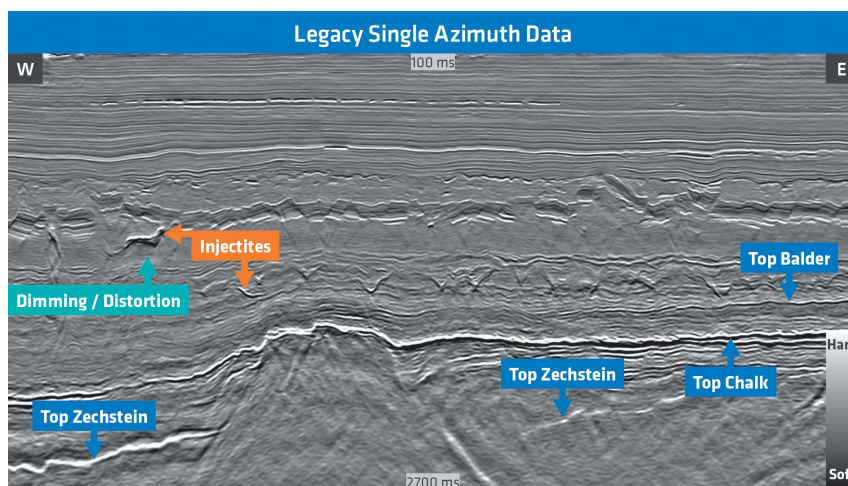

Figure 1 Legacy PSDM stack with single azimuth towed-streamer data and key geological elements.

used successfully in complex and challenging areas (Naumann et al., 2019). The multisensor streamers have been towed at depths between 25 and 28 m for better signal-to-noise ratio, especially at very low frequencies. The 2011 survey used a standard dual source configuration and was acquired in two phases with respectively 6 x 6000 m x 100 m and 10 x 6000 m x 75 m spreads.

Wide tow multi-source solutions have recently been evolving, with the number of sources and the distance between outer sources increasing continuously. In this dual/triple source case, the near-offset coverage and density may be considered insufficient to meet high-resolution standards for shallow imaging. However, adding all three directions to a joint near-offset regularization scheme proves to be efficient in reconstructing a reliable signal on a 6.25 m x 6.25 m spatial grid size, for offsets in the order of 50 m to 125 m. Indeed, the azimuth diversity is rather trivial for offsets close to zero, therefore allowing the acquisition efficiency to be optimized at the survey design stage, if all the azimuths are being considered. This solution effectively meets requirements for shallow hazards studies as well as shallow prospect identification where resolution and robust AVO are both critical. Figure 3 illustrates the high level of detail recovered with the combined near-offsets data, which could not be recovered by simple data interpolation within one sail line direction only. Both the MAZ design and the wide-tow elements were key factors in producing

the desired data sampling without sacrificing efficiency, though it is also worth noting that the inline minimum offset from the sources to the closest recording channels was reduced to about 65 m (for the new set-up), to guarantee a minimum coverage in each single vessel pass.

In the remainder of this article, we focus on the multi-azimuth aspects in processing and velocity model building, and the benefits for the final imaging steps and interpretation. The azimuth and offset diversity can be illustrated with rose diagrams which are presented in Figure 4 for all surveys plotted simultaneously assuming reciprocity. When evaluating the full offset range, it is obvious that the main illumination contributions are restricted to the three nominal sail line directions. However, when we focus our analysis on a short offset 0-2000 m range, which effectively covers the 0-40 degrees reflection angle range of the Top Balder to BCU interval (with a maximum depth below 2100 m in this area), the plots reveal that azimuthal information is available outside the three sail line directions courtesy of the wider-tow source configuration.

To take advantage of the richer azimuth information, we split the data into six reciprocal azimuth classes of 30 degrees, with every other azimuth class centre aligned with each of the three sail line directions. Note that the final classification of the data in x-y-offset-azimuth bins was ultimately achieved at the binning and regularization stage prior to the final Kirchhoff Pre-Stack Depth
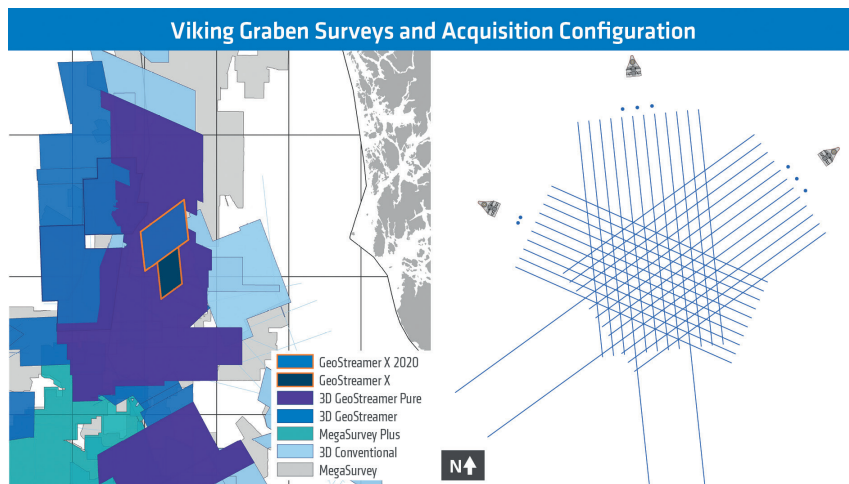

Viking Graben Surveys and Acquisition Configuration

GeoStreamer X 2020
GeoStreamer X
3D GeoStreamer Pure
3D GeoStreamer
MegaSurvey Plus
3D Conventional
MegaSurvey

N↑

Figure 2 Location of the 2019 survey and its extension in 2020 (left). On the right, the 2019 acquisition layout for the three directions is sketched with the legacy 2011 data in the NW-SE direction and the distinct 'long tails' streamers for the two new directions.
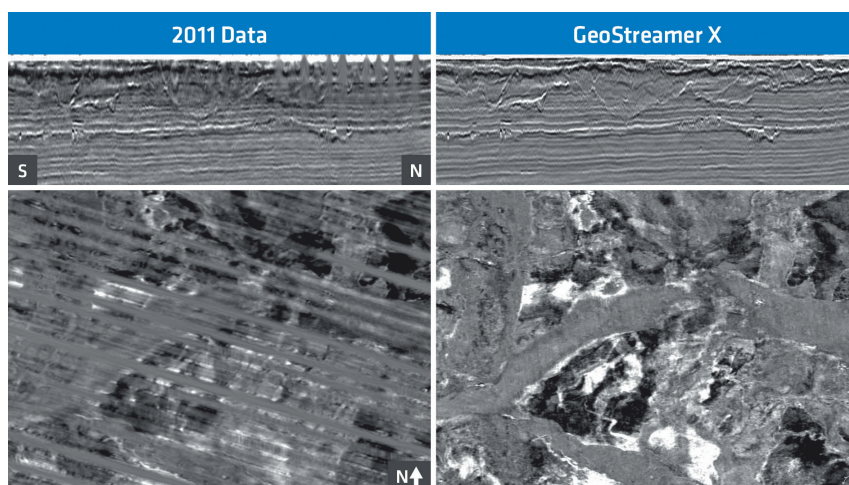

2011 Data

GeoStreamer X

S   N

N↑

Figure 3 Shallow seismic cross-sections (top), and time slice at 224 ms (bottom). The water-bottom reflection is at approximately 150 ms (TWT) in the area. The acquisition footprint is clearly visible on the 2011 data (NW-SE direction). Very near-offset data is lacking in the standard 3D seismic data and results in illumination gaps, which would not be recovered by simple data interpolation. Quaternary channels with internal geometry and a clear channel base are revealed in detail as well as underlying, possibly gas-filled sand mounds and minor scours or ploughmarks present in the volume.
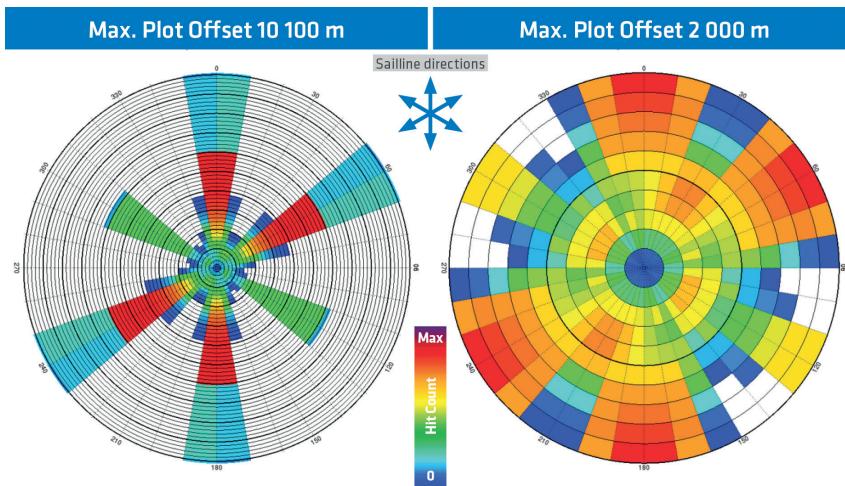
Figure 4 Rose diagram of the complete MAZ layout with the total offset coverage (left) and focus on the 0-2000 m offset range (right).

Migration (KPSDM) and was carried through post-processing. The actual results are shown in the last section of this article.

To achieve even higher operational efficiencies the 2020 extension programme employed an even wider source configuration and also used a wider streamer separation than the 2019 programme discussed here, resulting in even richer azimuth information in the short-to-moderate offset data.

Reducing turnaround with efficient pre-processing during acquisition

The following paragraphs describe the key pre-processing steps applied to the data up to and including demultiple, which were applied on individual sail line directions, in parallel with the acquisition itself.

For all multisensor streamer projects the recorded hydrophone and geosensor data go through 3D wavefield separation, which yields the up-going pressure wave field (P-UP), free of receiver ghosts (Carlson et al., 2007). A compensation for the source ghost in both phase and amplitude is applied before the designature process. A multi-domain and iterative solution for deblending the triple source data is applied to the two new datasets only, prior to the 3D source deghosting step which broadens the signal bandwidth. The subsequent designature step is as accurate as possible by making use of 3D directivity operators and recorded shot-by-shot source signatures (Tabti et al., 2018). Finally, the data are carried through linear noise and seismic interference attenuation prior to demultiple, on a need-to basis.

A comprehensive demultiple sequence was applied by combining model-based and data-driven multiple model generation to address both short and long period multiples. Short period surface-related multiples were attenuated using both wavefield extrapolation with a SWIM (Separated Wavefield Imaging) generated reflectivity model (Oukili et al., 2015) and a convolutional seabed modelled 3D SRME (Barnes et al., 2015). Longer period multiples were addressed using a combination of muted convolutional SRME and parabolic Radon demultiple. While the full integrity processing product involved the application of the complete processing sequence, only a subset of all processing steps were applied for the early out product for which a simpler designature process was selected and fewer multiple models were produced.

The methodology enables us to commence the pre-processing work after first shot, therefore substantially reducing the project turnaround time.

Utilizing rich offset and azimuth information to build the velocity model

The velocity model building stage (VMB) has a pivotal role in multi-azimuth imaging as it both benefits from the increase in subsurface information to produce a more accurate model, and contributes to the MAZ enhancement through the migration. Consequently, the VMB process in this study was revised to maximize the potential of the azimuthal information in Full Waveform Inversion (FWI) and tomography workflows.

In order to quantify any improvements to the estimation of velocities as derived from the MAZ survey, we will compare the new model to the velocity model that was derived from the 2011 data (Ciotoli et al., 2016). This legacy model was created in 2016 using single azimuth FWI and tomography. Although the technology and experience have evolved in the last four years, it is clear that both the longer offsets and richer azimuthal contributions were key in defining the final model. We demonstrate that a full velocity model can be generated with a great level of detail using exclusively data-driven methods, predominantly FWI.

The initial velocity model was derived from the 2016 model after a mild smoothing and the removal of high-velocity sand injectites, which were previously inserted mainly based on seismic interpretation. The smoothing is required to ensure better convergence of the FWI inversion process. In FWI, synthetic shot gathers are generated using the initial velocity. The difference (residual) between the acquired (observed) and synthetic data is used to update the velocity in order to minimize the residual. Since FWI is a non-linear inverse problem, it is solved in an iterative way where the updated velocity model is used for new synthetic shot generation and a new update. FWI uses both refractions and reflections to estimate the same velocity model, though the approach followed here is sequential (Figure 5).

The first FWI step used refraction data from 2 Hz up to 12 Hz for offsets up to 6 km. Despite the offset limitation, we could already observe an improved match between the forward modelled data and the recorded shots at longer offsets (> 6 km).

This step mainly introduced details in the shallow overburden, down to 1-1.5 km depth (depending on local gradients), where complexity is high due to the presence of channels, velocity inversions, mud diapirs and sand-injectites.

The second FWI step focused on the refraction data up to 15 Hz in the 'long tails' (two acquisition directions with up to 10 km offset). At this stage, the anisotropy models were adjusted as it globally reduced data misfits, thus providing a better starting point for FWI iterations with the very far offsets. Figure 6

shows the sensitivity kernel at 9 Hz from the two 'long tails' directions, which is created from a single inversion iteration and indicates where in the model space the data are sensitive to a velocity perturbation. The perturbation effectively illuminates the overburden down to the Top Chalk, and well underneath all the sand-injectites. This is true for both azimuths, therefore providing better coverage of the geological bodies and resulting in better lateral resolution in the velocity model.

The depth slices in Figure 7 show low velocity anomalies with a near-circular shape at about 1000 m depth, very well correlated with the reflection image and previously undetected. Preliminary interpretation suggests that these structures are likely to be mud diapirs (Løseth et.al., 2003) and indicate areas of possible overpressure. The velocity model can therefore be used as an attribute to identify drilling hazards. At this stage, the low wavenumber component of the cemented bodies (sand-injectites) has been updated and translates into an increase of velocity in the vicinity of the anomalies, though the accurate shapes and velocity values are mainly achieved at the later stages of the VMB. In summary, the long tails and multi-azimuth refraction FWI have contributed to both increased penetration depth and overburden accuracy.

Once the P-UP data after demultiple from the fast-track processing route were ready, the reflection data were included in the multi-azimuth FWI inversion. Using reflections increased the vertical resolution of the velocity model. It also added low wavenumber features below Top Chalk and down to the acoustic basement (deepest visible primary reflection), where subtle velocity inversions were expected. The final iteration of reflection FWI was run with an ad-hoc parametrization to solve the various velocities within the sand-injectites. Figure 7 shows the final velocity model overlaid on a stack where pull-up effects and focusing are improved at the Top Chalk reflection and deeper strata.

The subsequent mis-ties analysis was performed for every key horizon and confirmed a good match to available well data with a positioning error of less than 1% on average. No velocity calibration was needed but anisotropy was adjusted in order to centre the global gamma distribution around 1. Gamma is the measurement of residual move-out on image gathers, where a value of 1 represents flat gathers. Tomographic updates successfully narrowed the global gamma distribution, and also increased similarity between the distributions of each individual azimuth data.

The final reflection-based tomographic updates were run using the full integrity P-UP demultiple data. This tomographic
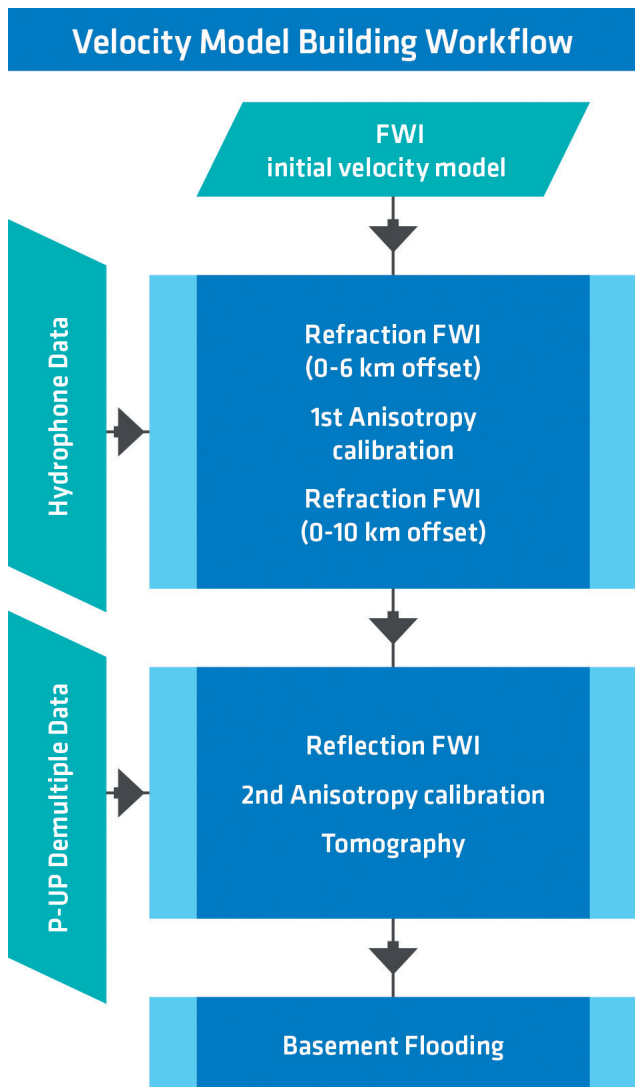

Figure 5 Flow diagram of the complete velocity model building work.
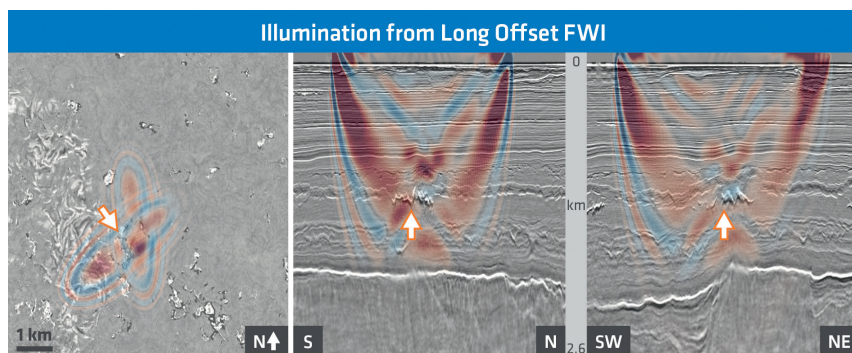

Figure 6 FWI sensitivity kernel at 9Hz for long offset refractions over sand-injectites highlighted in yellow. Depth slice (left), azimuth 1 (centre), azimuth 2 (right).
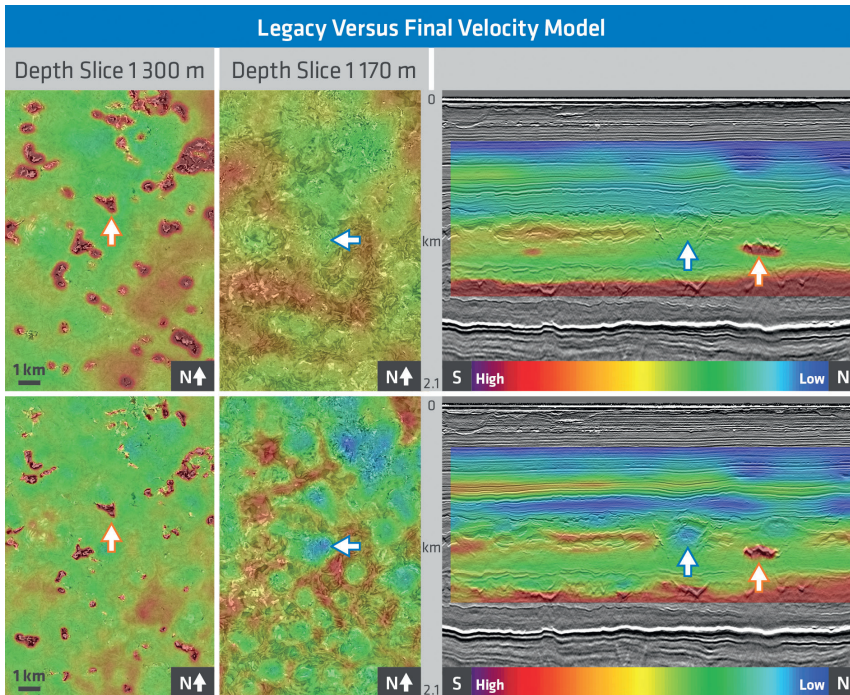
Figure 7 Comparison between fast-track full angle KPSDM stack migrated with colour overlay of the legacy velocity model (top) and full-integrity full angle KPSDM stack migrated with colour overlay of the final velocity model (bottom). Sand-injectites (orange arrow) and mud diapirs (blue arrow) are visible and better positioned in the final velocity model.

approach utilizes the same wavelet attributes computed using a pre-stack beam migration formulation (Sherwood et al., 2008) for a number of iterations. Data residuals after migration through a given velocity model, where each azimuth is tagged, are tomographically back-projected as slowness updates to the initial model (Sherwood et al., 2011). For the VMB purpose, only the three main azimuths were classified with offsets between 0 and 6000 m. In other words, residuals from the three main azimuths are simultaneously inverted to output a single velocity update that provides the best overall fit. The wavelet attributes allow the discrimination of poor RMO picks when a given azimuth does not provide illumination. This approach was used for three model building units (MBU) starting from Miocene down to the basement. For all three MBUs, the inversion smoothing filter was kept relatively large to avoid altering the shape of the details that were introduced at the FWI steps. Migrated gathers and gamma distributions were regenerated with the final pre-processed data for each azimuth, as a final flatness QC.

At the last step in the VMB workflow, the basement refractions, observed in the 'long tails' data, were utilized to derive smooth and spatially variable velocity values for the basement flooding.

Enhancing resolution and illumination with full azimuth imaging

As mentioned in the introductory section, all the datasets were regularized and migrated as one 5D multi-azimuth volume with six azimuth classes where the sampling supported it (offsets smaller than 2000 m). This means that we achieved a fundamental two-step improvement compared to traditional MAZ imaging. Firstly, the data coming from the three single vessel acquisition directions are all classified in offset and azimuth bins, instead of treating each sail line direction independently. Secondly, the azimuth bin size reduction from 60 degrees to 30 degrees implies that the signals coming from adjacent traces in the same azimuth class bin will be more similar and are less likely to interfere poorly in the migration step (commonly referred to as 'smearing') and in the presence of residual move-out, whether that is azimuthal-dependent or not.

In other words, the entire dataset is treated as a full azimuth survey (FAZ) within the relevant offset range in this area. Despite the many improvements and great detail added to the final migration model, it is fair to expect some residual misalignments in offset/angle gathers and between azimuth sectors. This strategy allows a proper optimization of the migrated pre-stack information, for both improved stacking response and resolution, as well as more reliable
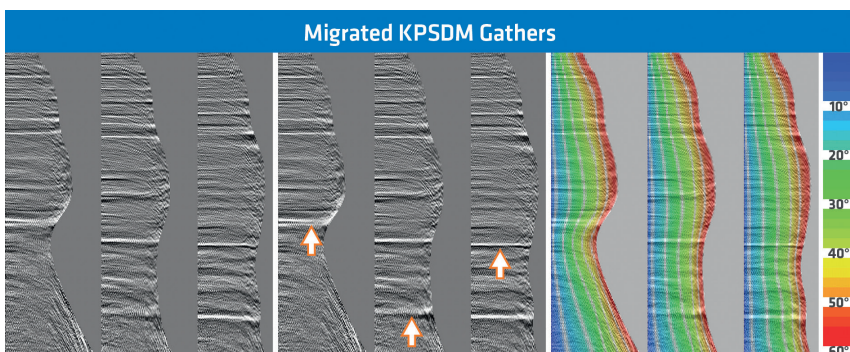

Figure 8 Common-Offset/Common-Azimuth (COCA) gathers (three) with various strata: raw migration output (left), after residual 5D event alignment (centre), the latter with true Walden angles of incidence overlay (right). The correction is small but noticeable at various depths. Note that some amplitude jitters are still expected as it reflects the difference in illumination between the azimuth classes. Arrows point to areas where the largest time shifts are observed and the reflectors appear clearer after correction on these type of displays.

quantitative interpretation, for example when deriving pre-stack AVO attributes. Note that the maximum vertical time shift that could be measured in the pre-stack data alignment step was in the order of +/- 5 ms, as illustrated in Figure 8.

Further coherency enhancement was achieved in the 5D pre-stack domain by attenuating both spurious amplitudes and coherent events that exhibit clear moveout in the offset or azimuth dimension, using both local slant-stack and Radon filters. Attention was put into not smearing true reflection events that may only appear in certain azimuth classes (Figure 9). For the same reason, the method chosen to produce the final MAZ image follows the selective stacking principle presented by Frolov et al.

(2016). Through local 5D analysis, the selection process excludes part of the gathers which do not contribute constructively to the total image, thereby improving the signal-to-noise ratio and preventing the dimming of strong reflections which may be poorly illuminated along certain azimuths.

Figure 10 illustrates the total gain achieved through the newly completed study, when compared to what could be achieved using the 2011 data alone. Illumination and resolution are greatly improved, also in areas that were seemingly fit for interpretation. In addition to the benefits already highlighted, we observe a significant reduction of a linear pattern on time slices, which is aligned with the 2011 acquisition direction, and identified as
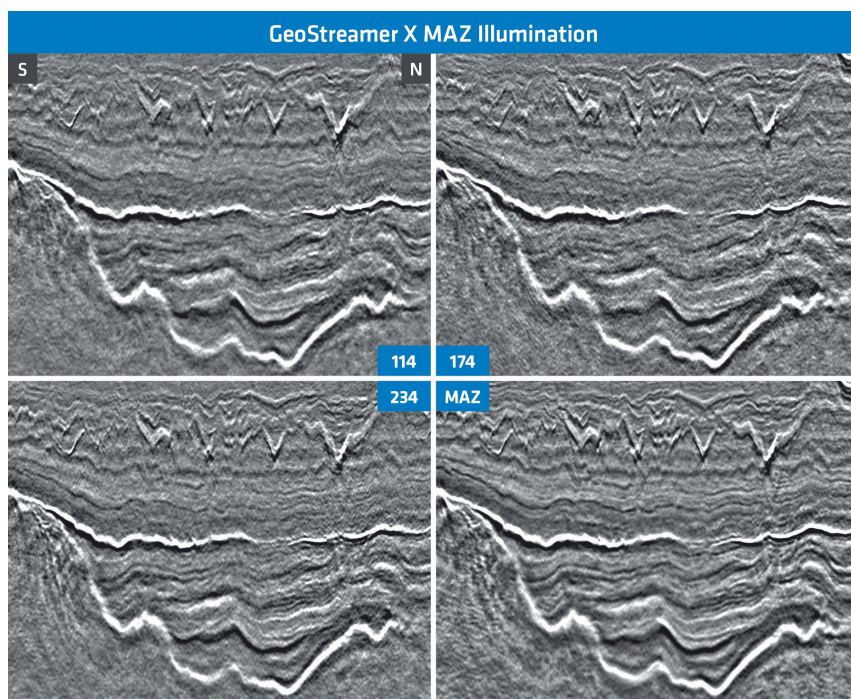

GeoStreamer X MAZ Illumination

Figure 9 Full angle KPSDM stack (0-40 degrees) sections of individual azimuth classes (114, 174 and 234 degrees) and selective MAZ stacking using all azimuth classes simultaneously. The MAZ stack shows both improved continuity and a greater level of detail.
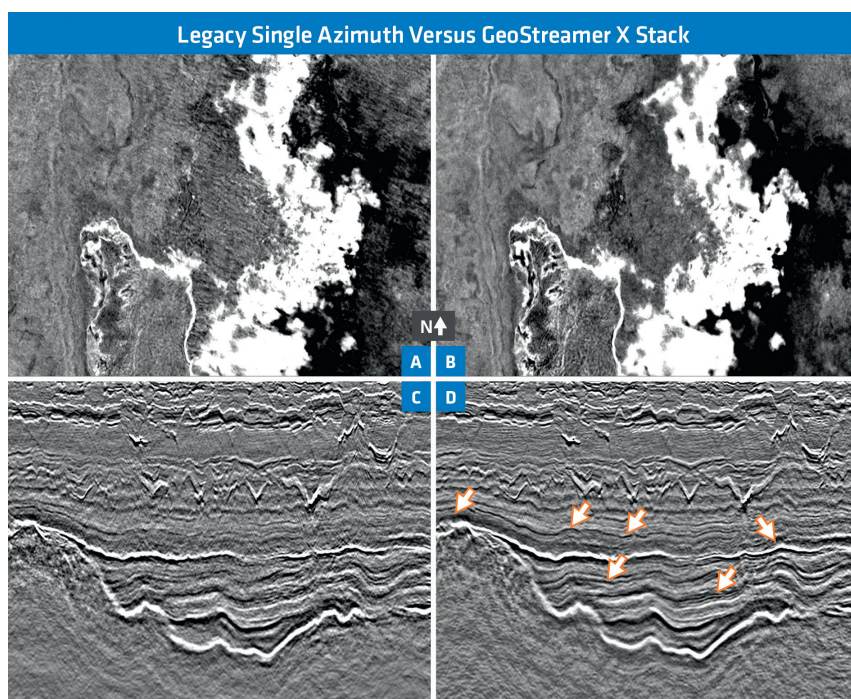

Legacy Single Azimuth Versus GeoStreamer X Stack

Figure 10 2011 single azimuth KPSDM stack (a, c) compared to the new KPSDM MAZ stack (b, d). Time slices (top row) cut through the Top Chalk reflection which is the rugose bright event in the centre of the cross-sections (bottom). Arrows in d) highlight improved key features in the MAZ stack.

migration artefacts of the poorly illuminated and rugose reflections on the cross-section. Note that this undesired imaging noise is much less noticeable in the single azimuth stacks of Figure 9. Indeed, in a standard 3D towed-streamer configuration, the true offset and azimuth distribution typically exhibit some sparse clustering which can result in suboptimal imaging of the most complex reflection surfaces. However, using a novel and comprehensive survey design approach, leveraging recent advances in towing techniques and imaging all the data in a true multi-azimuth manner, the interpretability of the final results is well above what could be expected from combining three overlapping images. Quantitative interpretation is currently underway and, so far, the early analysis confirms excellent seismic-to-well tie for the 10 wells available to us in the area.

Conclusions

The towed-streamer MAZ solution presented in this article is a first of its kind by being much more than just a set of three standard 3D streamer surveys. Further work will be conducted to quantify the benefits of the offset and azimuth diversity for the velocity model and the MAZ imaging workflows. Nevertheless, the total cost of this integrated study is considerably lower than that of the present-day estimates for alternative FAZ solutions (for example an ocean bottom seismic survey) while the turnaround is on par with the one expected of a standard single azimuth 3D towed-streamer acquisition and imaging project. While this project has challenged our ways of working, it has pushed us to use absolutely all of the recorded information and to produce a more complete picture of the subsurface both in the post-stack and pre-stack domains. The integration of the survey design study with the acquisition operations and the imaging technology has shown great flexibility in rapidly providing a fit-for-purpose solution, which we believe can be efficiently adapted to meet challenges in different geological areas.

Acknowledgements

References

Barnes, S.R., Hegge, R.F, Schumacher, H. and Brown, R. [2015] Improved shallow water demultiple with 3D multi-model subtraction. *SEG Internation Exposition and 85th Annual Meeting*, 4460-4464.

Carlson, D., Long, A., Söllner, W., Tabti, H., Tenghamn, R. and Lunde N. [2007] Increased resolution and penetration from a towed dual-sensor streamer, *First Break*, **25**, 71-77.

Ciotoli M., Beaumont S., Oukili J., Korsmo Ø, O'Dowd N., Rønholt G., Dirks V. [2016] Dual-sensor data and enhanced depth imaging sheds new light onto the mature Viking Graben area. *First Break*, **34**, 73-79

Frolov, S., Brown, S., Arasanipalai, S. and Chemingui, N. [2016] Post-migration image optimization: a Gulf of Mexico case study. *SEG International Exposition and 86th Annual Meeting*, 4695-4699.

Løseth, H., Wensaas, L., Arntsen, B. and Hovland, M. [2003] Gas and fluid injection triggering shallow mud mobilization in the Hordaland Group, North Sea. In: Vasn Rensbergen, P., Hillis, R.R., Maltman, A.J. and Morley, C.K. (eds) Subsurface Sediment Mobilization. *Geological Society, London, Special Publications*, **216**, 139-157.

Naumann, S., Widmaier, M. and Rønholt, G. [2019] Novel variable streamer length acquisition tailored to Full Waveform Inversion and high resolution imaging. *81st EAGE Conference and Exhibition*, Extended Abstracts, We_R04_06.

Oukili, J. , Jokisch T., Pankov, A., Farmani, B., Ronhølt, G., Korsmo, Ø., Raya, P.Y. and Midttun, M. [2015] A novel 3D demultiple workflow for shallow water environments – a case study from the Brage field, North Sea. *77th EAGE Conference and Exhibition*, Extended Abstracts, N114.

Tabti, H., Wisløff, J.F., Høy, T. and Widmaier, M. [2018] Shot to Shot Source Signature Variation Correction. *80th EAGE Conference and Exhibition*, Extended Abstracts, Tu_E_05.

Sherwood, J., Sherwood, K., Tieman, H. and Schleicher, K. [2008] 3D beam pre-stack depth migration with examples from around the world. 78th SEG Annual Meeting, Expanded Abstracts, 438–442.

Sherwood, J., Jiao, J., Tieman, H., Sherwood, K., Zhou, C., Lin, S. and Brandsberg-Dahl, S. [2011] Hybrid tomography based on beam migration. 81st SEG Annual Meeting, Expanded Abstracts, 3979–3983.

Widmaier, M., O'Dowd, D. and Roalkvam, C. [2019] Redefining marine towed-streamer acquisition. *First Break*, **37**(11), 57-62.

Widmaier, M., O'Dowd, D., Roalkvam, C., Ciotoli, M. and Limonta, L. [2020] Addressing imaging challenges in the Viking Graben with multi-azimuth acquisition, longer offsets, and wide-tow sources. *SEG International Exposition and 90th An*nual Meeting.